

# THE 4TH INTERNATIONAL CONFERENCE ON ALUMINUM ALLOYS

## A DSC AND TEM INVESTIGATION ON A 2014+20%Al<sub>2</sub>O<sub>3</sub> COMPOSITE

G. Riontino<sup>1</sup> and A. Zanada<sup>2</sup>

1. Dipartimento di Chimica Inorganica, Chimica Fisica e Chimica dei Materiali, Unità INFM, via P. Giuria 9, 10125 Torino, ITALY

2. Alures, ISML, via Bovio 6, 28100 Novara, ITALY

### Abstract

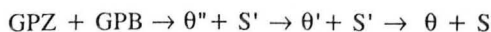
DSC and TEM analysis have been performed on a powder metallurgy 2014+20%Al<sub>2</sub>O<sub>3</sub> discontinuous fibres composite and the relative unreinforced alloy in the natural and artificially aged state. An overall analogous behaviour have been evidenced for both the materials with a slight enhancement of the precipitation kinetics in the composite. Differences in the relative amount of the main precipitation signals, corresponding to the S' and  $\theta'$  formation, have been interpreted on the basis of a higher dislocations concentration in the composite and of a limited Mg reaction at the fibre-matrix interface.

### Introduction

The thermal treatments for aluminium matrix composites (AMC) must be elaborated with particular care, on the basis of conventional treatments on the unreinforced alloys, taking into account some different behaviours during ageing.

The typical differences between the composite and the master alloy are essentially related to the precipitation kinetics of the hardening phases [1,2] and to the overall gain in mechanical properties; in some cases a partial ageing suppression may be evidenced [3,4]. Accordingly, two features are generally reported in literature. Firstly, variations in the dislocations concentration and consequently in the lattice vacancies content: these elements, acting as nucleant of the hardening phases, determine different ageing response [2,5]. Secondly, chemical activities at the fibre-matrix interface, regarding in particular reactions of some alloying elements, lead to a depauperation of the matrix in the final ageing [3,4,6].

Hardening during conventional thermal treatments of the Al-Cu-Mg-Si 2014 alloy object of the present study is based essentially on the formation of S' orthorhombic CuMgAl<sub>2</sub> precipitates with the copresence of  $\theta'$  tetragonal CuAl<sub>2</sub>. Moreover, other particles types could also form during ageing, as reported in literature [7,8]. In particular, the  $\theta'$ -phase forms when the ratio Cu/Mg is higher than 4. In this case the precipitation sequence results to be:



Each phase nucleates and grows both on vacancies and on dislocations, or develops from precursors; the different defects concentration in the composite with respect to the monolithic

alloy may influence the transformation path during annealing.

Aim of the present work is to investigate the precipitation sequence and its possible modifications into the composite with respect to the monolithic material submitted to the same preliminary treatments.

A microcalorimetric investigation (DSC) has been performed, together with TEM observations on samples both naturally and artificially aged.

### Materials and Methods

Materials have been prepared at ISML via powder metallurgy technique, starting from prealloyed 2014 powders (wt. % composition: 4.3Cu, 0.85Mg, 0.94Si, 1.02Mn, 0.18Fe, 0.03Zn, 0.03Ti), mixed to a 20% in volume of  $\delta$ -Al<sub>2</sub>O<sub>3</sub> discontinuous fibres, cold compacted, hot sintered and extruded in bars. Slices about 2 mm thick, perpendicular to the extrusion direction, were then cut and solutioned at 502°C for 2 hours, water quenched and artificially aged at 170°C for different times, after 24 hours at room temperature. Disks 6 mm in diameter were punched from slices for DSC measurements in a DuPont 910 thermal analyzer. Specimens for TEM have been electrochemically thinned in CH<sub>3</sub>OH+HNO<sub>3</sub> (3:1 in volume) at -30°C and observed by an analytical Jeol 2000EX.

### Results and Discussion

Thermograms at the same scanning rate for the monolithic and the composite in the T4 state (natural ageing for some months) are reported in figure 1.

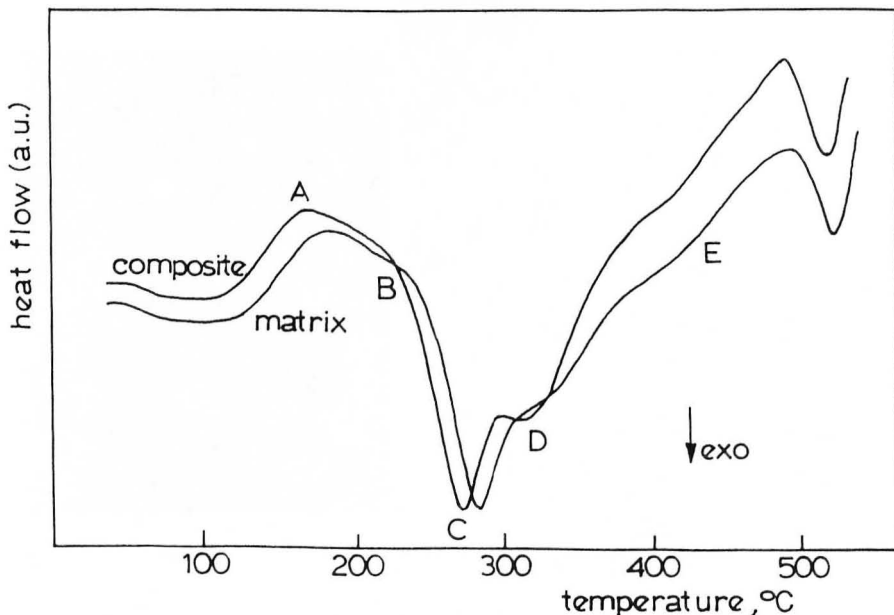


Figure 1. Thermograms for composite and matrix after natural ageing (T4 state) at a scanning rate of 30 K/min.

At a first look, the trend of the thermograms appears to be qualitatively similar, and four ranges of temperatures may be evidenced:

- below 130°C, a small exothermal peak, relating to clustering phenomena, is apparent;
- in the range 130-230°C an extended endothermal effect may be outlined; it originates two peaks "A" and "B", to be assigned to the dissolution or a partial reversion of precursor phases formed during ageing at room temperature;
- between 230°C and 350°C a wide exothermal signal occurs, in which two peaks "C" and "D" can be individuated;
- at higher temperatures, a complex endothermal signal "E" takes place, preceding a small eutectic melting at temperatures near the solutioning one.

Due to the similarity of the DSC signals for the two materials, one can deduce that during preparation and solutioning of the composite possible reactions of the matrix elements with the reinforcement do not take place in a relevant way so to alter substantially the successive precipitation sequence. The presence of the precipitation exothermic peaks C and D suggests that essentially two of the phases into which the 2014 alloy may decompose are forming during the calorimetric scan.

A detailed TEM analysis on specimen isothermally aged at various temperatures and times, in correspondence of a slightly underaged, peak aged and overaged state referring to hardness curves elsewhere reported [9], shows the co-presence of  $\theta'$ -platelet and S'-needle particles, these last being the main precipitate (figures 2 and 3).

S' formation have been observed to occur essentially prior to  $\theta'$ , so the peaks C and D have been assigned to S' and  $\theta'$  precipitation respectively, according to literature data [10].

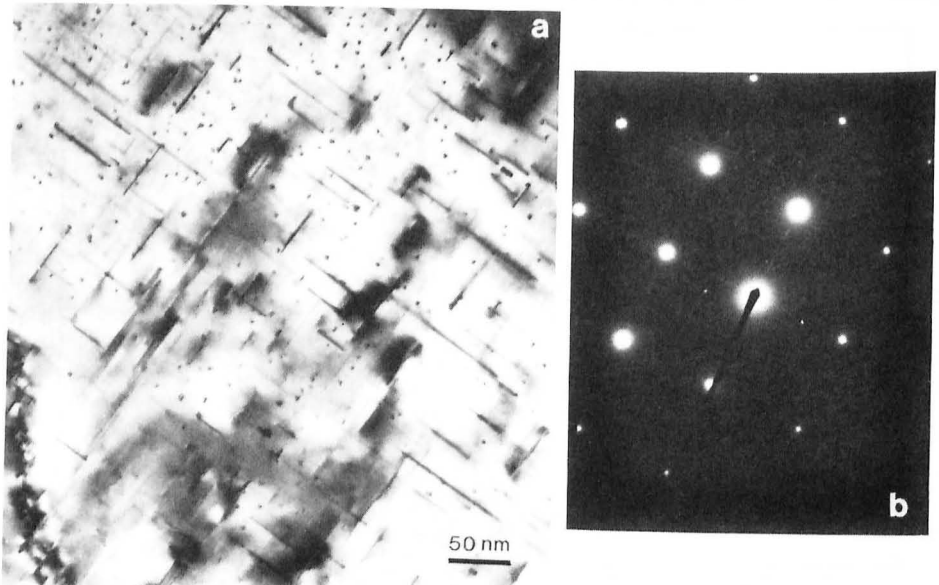


Figure 2. a) S' dominating microstructure in peak-aged monolithic alloy, zone axis [100]; b) electron diffraction of microstructure in a): coherency streaks through  $\{200\}$  and  $\{220\}$  matrix spots should be attributable to some amount of the precursor  $\theta''$ .

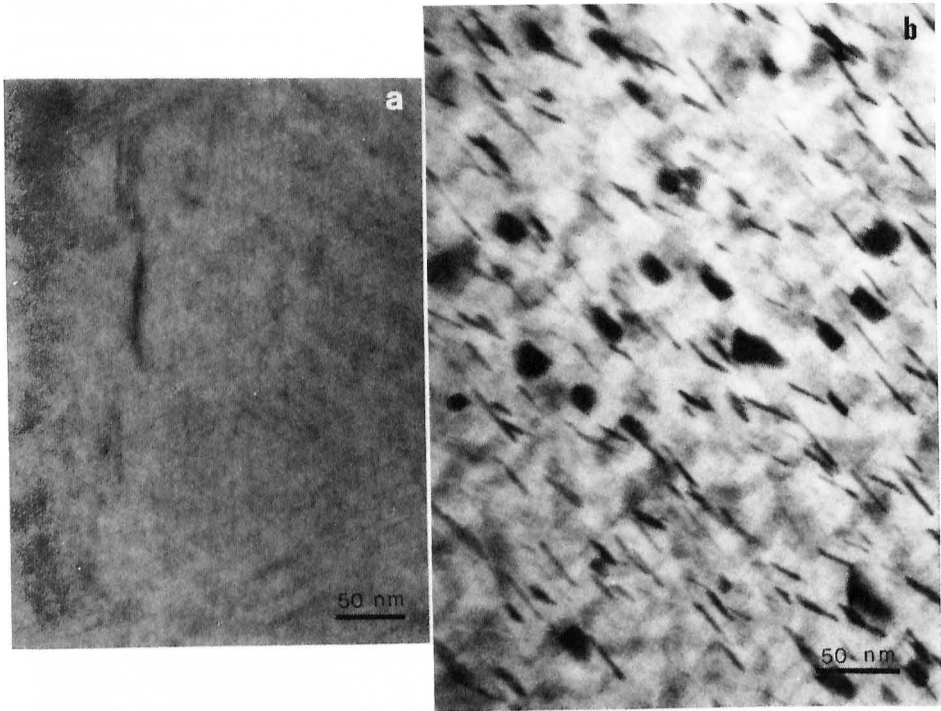


Figure 3. a) S'-needle particles in peak-aged monolithic alloy, zone axis close to [211]; b) S'-needle +  $\theta'$ -plate particles in slightly overaged AMC.

A more detailed analysis of the thermograms in figure 1 shows a slight decrease (from 2 to 10°C) of the peak temperatures of all the transformations for the composite with respect to the monolithic. This is a well known characteristics reported in literature for other composites [2,5] and it is attributable to a higher dislocation density in the reinforced matrix, which act as centres of heterogeneous nucleation and enhance the diffusion of solute atoms in the corresponding matrix, so producing a faster precipitation in the composite. In effect, as can be seen in figure 4a, an extended network of dislocations is observable in the composite, more concentrated close to the fibres. Consequently, a gradient in dislocations concentration conditions the local distribution of precipitates [11].

A further consideration can be made as regard the quantitative contribution of the main precipitation peaks C and D to the overall exothermic signal. In the composite, a decreased amount of the S'-phase (peak C) with respect to  $\theta'$  (peak D) is observable as compared to the analogous signals in the matrix. This could be explained both by a preferred heterogenous formation of  $\theta'$  on dislocations and partially by a slightly decreased Mg concentration, due to its reaction at the interface with the fibres. Actually, TEM observations (figure 4b, c, d) reveal the presence of  $MgAl_2O_4$  spinel particles, which subtract a limited quantity of Mg for the successive precipitation.

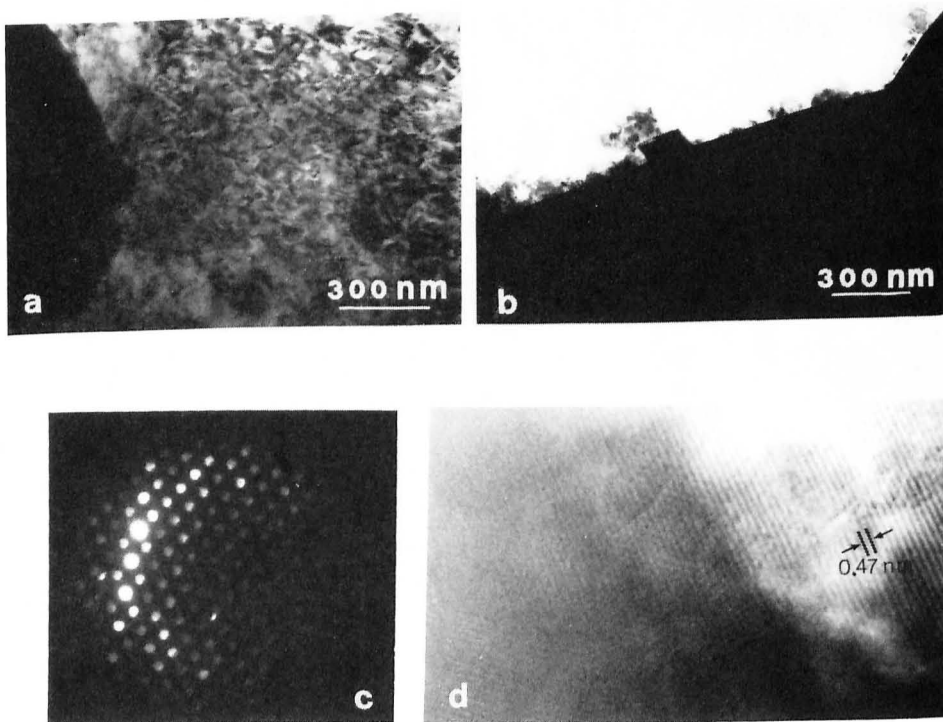


Figure 4. a) dense dislocations network extended in the AMC matrix originated by the  $\text{Al}_2\text{O}_3$  fibre shown on the left; b) TEM micrograph of  $\text{MgAl}_2\text{O}_4$  spinel particles developed on  $\text{Al}_2\text{O}_3$  fibre surface; c) convergent-beam electron diffraction of a spinel particle with zone axis close to  $[110]$ ; d) high-resolution electron micrograph of the particle, showing the  $\{111\}$  planes of the spinel, 0.47 nm apart.

To give a better insight into the main precipitation sequence, an artificial ageing at  $170^\circ\text{C}$  for times up to 120 hours has been performed on both the monolithic and the composite, prior to the DSC measurements. These latter are respectively shown in figure 5 a) and b) at a same scanning rate, together with the T4 thermograms for comparison.

The evolution of the thermograms is substantially the same for the two samples. According to TEM observations, during the first ageing times the  $\text{S}'$ -phase forms preferentially: the C-peak associated to its precipitation during the DSC scan is less evident than for the T4 state, it is very low after 4 hours and it disappears completely after 8 hours. The D-peak associated

to  $\theta'$ -precipitation decreases in intensity less evidently than C and it is present even after 16 hours of ageing. At the highest ageing times, only endothermic signals can be evidenced, indicating the dissolution of all precipitates formed during ageing.

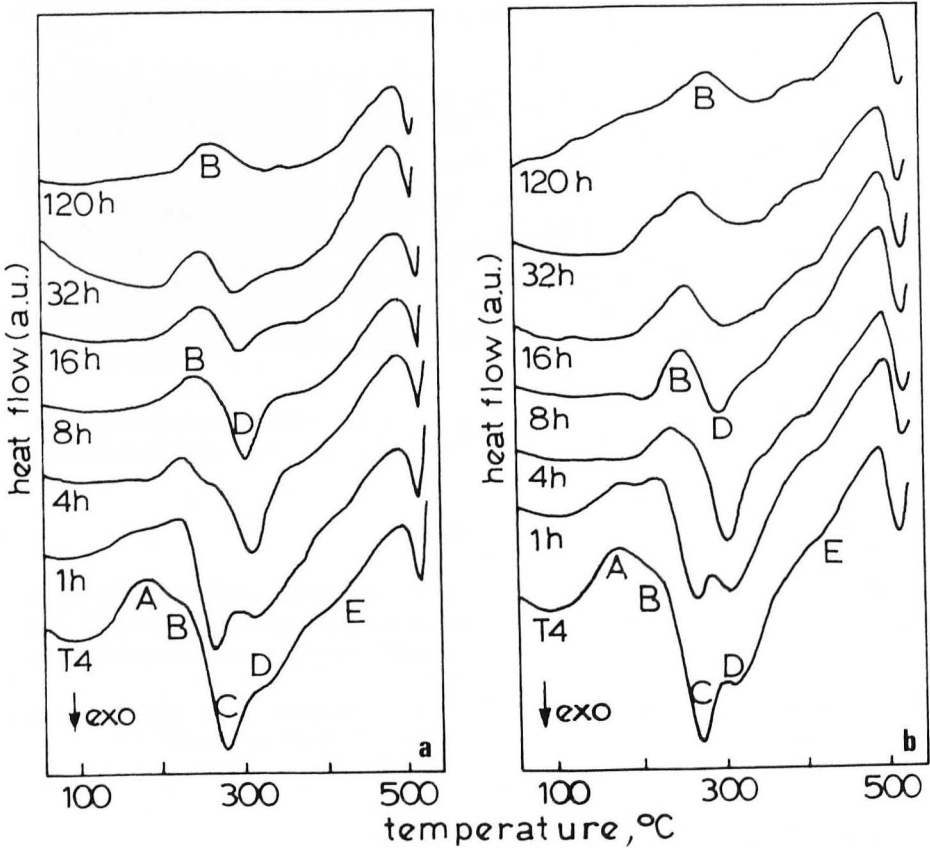


Figure 5. Thermograms for monolithic (a) and composite (b) after ageing at 170°C for the times indicated. Scanning rate: 30 K/min.

The same considerations can be made for the composite, in which the progressive disappearance of the C-peak is faster than in the matrix and the  $\theta'$  precipitation peak results more marked than in the monolithic material. This confirms that a preferential precipitation of S' takes place in the first stages of ageing and that  $\theta'$  forms with a higher volume fraction, selectively promoted by the higher dislocation density in the composite. The enhanced precipitation kinetics deduced by DSC for the composite, both naturally and artificially aged, is consistent with the accelerated ageing observed on the basis of hardness curves, TEM observations and other DSC data elsewhere reported [12,13].

In particular, it is to be remarked that differentiation in ageing response starts since the early stages. As an example, figure 6a) and b) shows respectively a well developed microstructure of coherent particles nucleated both homogeneously and heterogeneously in the composite artificially aged for short times and only small homogeneous clusters in the monolithic, this last well detectable in the lattice fringes image of figure 6c.

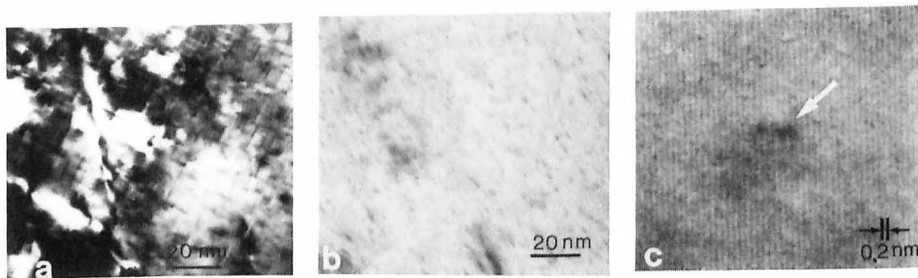


Figure 6. a) and b) microstructure at early stage of ageing in composite and monolithic, respectively; c) perturbation indicated by arrow in Al (200) lattice fringes image attributable to a small cluster in monolithic material.

### Conclusions

- The precipitation sequence in monolithic 2014 alloy and in the composite with  $Al_2O_3$  continuous fibres, both naturally and artificially aged, is essentially the same, based on  $S'$  and  $\theta'$  formation; a slightly different contribution of  $S'$  and  $\theta'$  on the overall precipitation has been evidenced in the AMC as compared to the monolithic.
- An enhanced kinetics of phase transformations can be envisaged in the composite with respect to the monolithic, due to a higher dislocation density produced by the fibres.

### References

1. R.D. Schueller and F.E. Wawner, J.Mat.Sci. **26**, (1991),3287
2. S.I. Hong and G.T. Gray III, Acta Metall et Mater. **40**, (1992), 3299
3. H. Ribes and M. Suery, Scripta Metall. **23**, (1989), 705
4. F. Pinna and E. Di Russo, Aluminium Alloys, New Process Technology, (Marina di Ravenna, Italy: AIM, Milano, 1993), 31
5. T. Christman, A. Needelman, S. Nutt and S. Suresh , Mat.Sci and Eng. **A107**, (1989),49
6. D.J. Lloyd, 2<sup>nd</sup> Int.Summer School on Aluminium Alloys Technology (Trondheim, Norway: NTH, 1993)

7. L.F. Mondolfo, Aluminum Alloys, Structure and Properties (Butterworths, London, 1976), 497, 644
8. R.D. Schueller, A.K. Sachdev and F.E. Wawner, Scripta Metall. et Mater. 27, (1992), 617
9. P. Fiorini, "Materiali Compositi a Matrice di Alluminio" (Alures-ISML Report 90/27808, Novara, Italy, 1990)
10. I. Dutta and C.P. Harper, Aluminium Alloys, their Physical and Mechanical Properties, ed. L.Arnberg et al. (Trondheim, Norway: NTH-Sintef, 1992)
11. P.B. Prangnell and W.M. Stobbs, Metal Matrix Composites-Processing Microstructure and Properties, ed. N.Hansen et al. (RISO Int.Symp. on Mater.Sci., 1991), 603
12. A. Zanada, Atti XVIII Congresso SIME di Microscopia Elettronica, (Padova, Italy: Microscopia Elettronica, suppl. n.2, 1991), 141
13. F. Garetto, undergraduate thesis, Torino University, Italy (1993)